Brake system model reduction for squeal noise study

S. Nacivet[1], O. Fazio[1,2], and J-.J. Sinou[2]

1 - PSA Peugeot Citroën, Centre technique de La Garenne Colombes, 18 rue des Fauvelles, 92250 La Garenne Colombes, France

2 - Laboratoire de Tribologie et Dynamique des Systèmes, UMR CNRS 5513, Ecole Centrale de Lyon, 36 avenue Guy de Collongue 69134 Ecully Cedex, France

samuel.nacivet@mpsa.com, olivier.fazio@mpsa.com, jean-jacques.sinou@ec-lyon.fr

Abstract*: Although the problem of friction-induced vibration has been the subject of many investigations over recent decades, it is still responsible for a large number of nuisances in the field of automotive. Using Abaqus For CATIA V5 (AFC) and Abaqus, this study presents a numerical process based on modal reduction to generate a Super-Element for the whole brake system. The size of the model is minimized using a specific non-linear modeling at the frictional interface. Then, the Super-Element is used in Matlab to check is ability to predict the stability analysis of large Finite Element Models that correspond to real automotive braking systems subjected to friction-induced vibrations. The effect on squeal instabilities (i.e the frequencies and the associated positive real parts) of the number of contact nodes at the frictional interface is investigated in order to reach a high-quality estimation with the smallest number of DOF possible. What could be improved in AFC and Abaqus to make the Super-Element more representative and easier to create is discussed. To finish, the limitation of a determinist point of view is illustrated.*

Keywords*: Vibration, Friction, Squeal, Reduction, Super-Element.*

1. Introduction

The problem of brake squeal in automotive was a subject of great interest for many researchers. Despite its limitations, a well appreciated method in industry consists to perform a Complex Eigenvalue Analysis (CEA) on the linearized system in order to predict the squeal propensity of the brake in a given frequency range (“Sinou, 2010”). For others methods in time (“Vermot des Roches, 2011” & “Loyer, 2012”) or in frequency domain (“Coudeyras, 2009”), taken nonlinearities into account, the system size becomes a huge problem since computation time and data storage can become very expensive.

Therefore, some researchers proposed to develop reduced models when Finite Element Models are considered in order to reduce the computational times. The most widespread reduction method in industry is the Craig-Bampton method ("Craig, 1987"). One of the major limitations for brake system and the squeal prediction is associated with the size of interface matrices due to the explicit use of the degrees of freedom at interface. Recently, performances of some others reduced bases built from the component modes or the real coupled modes have been tested by "Brizard, 2011" for the stability analysis of a disc/pads system in sliding contact. They proposed some enriched bases to improve the precision on the calculated complex modes and eigenvalues. "Loyer, 2012" developed also spatial model reduction with different kinds of reduction bases to approximate the non-linear vibrations of a TGV brake system. In these studies, all the physical contact degrees of freedom are kept. "Vermot des Roches, 2011" proposed parametrized reduction called the Component Mode Tuning method (CMT) that use the components free/free modes as explicit degrees of freedom in order to perform non-linear time simulations. Finally, some researchers discussed on the possibility to reduce the size of the frictional interface that is one of the main drawback of the classical use of the Craig-Bampton approach ("Villard, 2012", "Fazio, 2015").

In the present paper, the main results of "Fazio, 2015" are shown and current limitations are discussed. The Super-Element of brake system is evaluated according to CEA results. Notice that the interest of using CEA is only to validate the Super-Element according to it. Future works will attach to use the Super-Element with others kind of analyses to take advantage of the Super-Element size on computation time.

The paper is organized as follows: firstly, the brake system under study is presented. Secondly, the proposed reduction method and the global strategy for the generation of the reduced non-linear interface are discussed. More precisely the Super-Element creation and assembly are detailed. Thirdly, application for an industrial representative Finite Element Model is proposed. The efficiency of the reduction strategy is undertaken by performing a stability analysis around a non-linear equilibrium point for two level of reduction at the disc/pads contact interfaces. Finally, the limitation of a determinist point of view is illustrated by sensitivity observations for another industrial model.

2. The brake model under study

For this study a Finite Element Model of an industrial brake system that has been developed in Abaqus For CATIA V5 is considered. It can be decomposed in several parts as detailed in Figure 1-a. This system uses a floating caliper technology. The caliper that holds the two brake's pads can move with respect to the disc, along a line parallel to the axis of rotation of the disc. During a brake operation, hydraulic pressure is applied on the piston, which pushes the inner brake pad until it makes contact with the disc. Then, reaction force pulls the caliper body with the outer brake pad against the other side of the disc. Considering the Finite Element Model, a volume mesh is realized using 10-nodes quadratic tetrahedron (see Figure 1-b). It represents a total of 176956 nodes for 100710 elements.

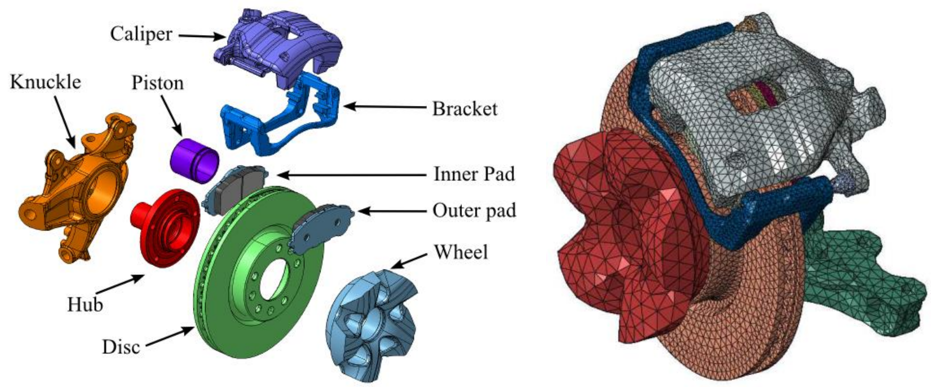

(a) Exploded view (b) Finite Element Model

Figure 1: Brake system details.

Contact and friction modeling are key parameters for squeal simulation. Here, *CONTACT PAIR card is used for node to surface contact modeling. The principal components of the brake system in contact with the pads are the disc, the piston, the caliper and the bracket. For all these contacts, pads are always defined as slave parts.

A linear penalty method is used for the contact constraint enforcement and the classic Coulomb's law is used for all the frictional interfaces. Also depending on the contact considered, separation can be taken into account or not. All these parameters are summed up in Table 1.

Contact	Friction coefficient	Separation
Disc/Pads	0.5	Yes
Piston/Pad	0.15	No
Bracket/Pads	0.15	Yes
Caliper/Pad	0.15	No

Table 1: Contact modeling

3. Model reduction method

Previous research works were carried out to define a model reduction method to apply stability analysis on industrial representative models (“Brizard, 2011” & “Vermot des Roches, 2011”). Alternatively, in continuity of “Coudeyras, 2009” and “Villard, 2012” works, “Fazio, 2015” used a Super-Element (SE) with a reduced contact interface. Various improvements have been made on the contact interface reduction step to be more representative.

First of all, it must be noted that the proposed strategy and reduction formulation is not compatible with the *CONTACT PAIR card used for contact in Abaqus due to the fact that the methodology involves node-based surface creation which cannot be defined as the master surface of a contact pair in Abaqus. One solution could be to directly define node to node contact between reduced nodes of both side directly in Abaqus with *GAP elements with friction. However, this strategy does not allow us to generate unsymmetrical terms in matrices using *MOTION which is the key point for stability analysis. So we decided to create reduced contact nodes only for the pads: coincident nodes on the disc volume mesh are imposed and a node to surface formulation with *CONTACT PAIR card is kept. The reduced contact nodes and their coincident nodes on disc mesh will then be used for condensation and node to node contact will be defined later in Matlab between them.

This section will describe the main steps in detail, but it is interesting for the reader comprehension to first sum up the whole process. Firstly, reduction points are defined in CATIA V5 and are used as constraints on disc only to have nodes at these locations. Abaqus for CATIA V5 is then used to generate the Abaqus input file. Using reduction points information, the Abaqus input file is modified to introduce reduced contact interfaces at the disc/pads interfaces with reduced number of nodes on both contacts sides of pads and disc that will be later used for condensation and node to node contacts. Secondly, the static equilibrium is computed on this Abaqus model with reduced contact interfaces. Then, deactivating the disc/pads contacts while fixing the displacement of the nodes of these reduced contact interfaces observed at the static equilibrium allows generating a Super-Element which is a linearization of this equilibrium configuration.

Node to node contacts are then used in Matlab at the disc/pads interfaces when the Super-Element (SE) is used to compute stability analysis with a new cubic contact law for the disc/pads interfaces. The global strategy is resumed on Figure 2.

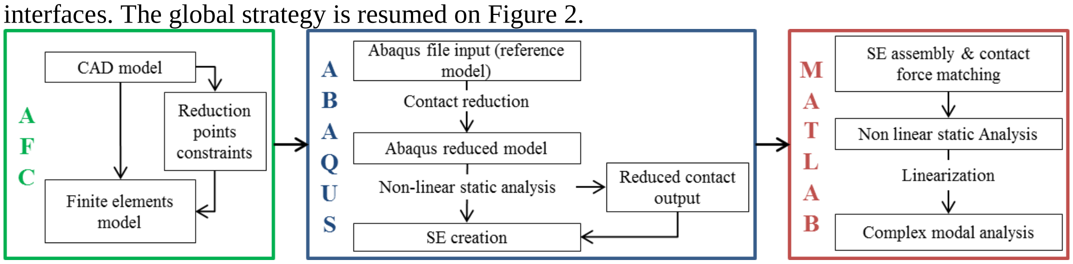

Figure 2 : Global strategy

The Abaqus for CATIA V5 (AFC) part is not detailed in this paper, this section is organized as follows. First the simplified contact modeling will be explained. Then, the Super-Element creation will be detailed to give some information concerning the Super-Element assembly and more particularly the method used to define contact force in the node to node contact.

3.1 Simplified contact modeling

As proposed by "Fazio, 2015", the idea is to reduce the disc/pads contacts defining node to node contacts with a limited number of nodes which will be later used as reduction nodes for the Super-Element creation. All the other interfaces are then linearized. This choice avoids adding errors from the reduction of multiple contact interfaces. In so far as the reduction of the number of nodes involved in contact must not affect the static solution "Villard, 2012" suggests to distribute the contact forces around these reduced contact nodes. The *DISTRIBUTING and *COUPLING options are therefore used in Abaqus. Figure 3 illustrates the contact modeling.

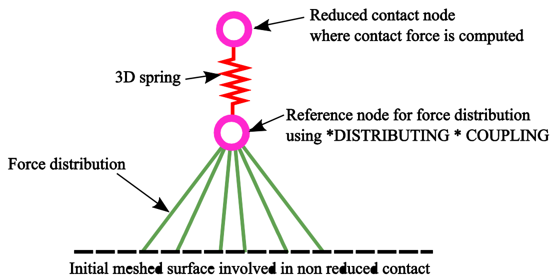

Figure 3: The reduced contact model.

An additional spring with arbitrary stiffness (i.e. the value of this spring is assumed to be very superior to the local stiffness) allows to link the reference node (which is slave in the distributing coupling) to the reduction node used for Super-Element creation. For the reader comprehension, it can be noticed that these nodes have the same geometric position in the model but they are dissociated on Figure 3 for a better illustration of the reduced contact modeling.

"Fazio, 2015" determined the best set of *DISTRIBUTING and *COUPLING cards parameters to limit the error induced by the reduction of disc/pads interfaces in the case of an isometric repartition of reduced contact nodes.

By default, using *DISTRIBUTING and *COUPLING cards to couple a single node to a meshed surface transfers the forces computed at the reference node to all the nodes of the meshed surface. An interesting option is to limit the distribution in a spherical region centered on the reference node by defining a radius of influence. In this case, referring to "Abaqus Users Manuel" the forces computed at the reference node are distributed only to the nodes of the surface that fall inside this spherical region. Another interesting parameter is the control over transmission through weight factors specified at each coupling nodes which allows the forces transferred to the coupling nodes to vary inversely with the radial distance from the reference node.

For the proposed contact reduction, the radius of influence and weighting method are the main parameters to be fitted in order to have a smooth variation of contact force over the coupling nodes.

In Abaqus 6.10 the influence of the mesh size is also taken into account in the weighting factor computation but it was not considered in this study. To facilitate the understanding of the present study, the classic polynomials defined below as weighting method will be used

$$w_i = 1 - \frac{r_i}{R}$$

$$w_i = 1 - \left(\frac{r_i}{R}\right)^2$$

$$w_i = 1 - 3\left(\frac{r_i}{R}\right)^2 + 2\left(\frac{r_i}{R}\right)^3$$

where r_i is the distance between the reference node and the i^{th} coupling node, R the radius of influence and w_i the weight factor computed.

As said before, reducing the number of contact nodes and distributing force must not affect the contact force mapping on the interface. Indeed it is not recommended to concentrate the forces at the vicinity of the new reduced contact nodes and thus to modify the static equilibrium. Considering these three weighting methods it is interesting to find for each of them the best radius of influence in order to ensure an uniform contact force distribution that matches the most with the initial non-reduced contact. As distribution is made in a circular region centered on the reference node, it is interesting to define the reduced contact nodes group as an isometric grid to reduce voids in distribution Figure 4. This isometric grid has been oriented using surface inertia.

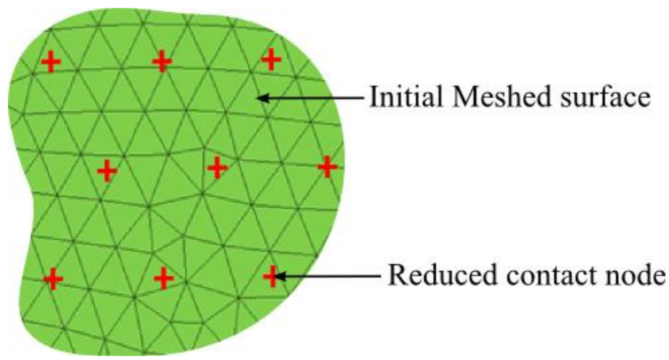

Figure 4: Reduced contact nodes layout.

Thus optimal radius will depend on the triangle size of the isometric grid. So the optimum was calculated for an academic example of a simple triangle of three nodes representing the elementary pattern of our isometric grid. Weighting coefficient mapping inside this triangle of reduced nodes is computed in Matlab for a triangle length of $1mm$. As an equal force on each node of the triangle is applied, the optimal radius that offers an homogeneous force distribution has to be found for each weighting method, which means a computed weight factor centered on 1 inside this triangle. Results are given on Figure 5 and Table 2.

It seems interesting to use a cubic distribution that offers the smallest standard deviation. Whatever the number of reduced contact nodes and so the size of the triangle chosen later in our reduction it will be easy to find, proportionally to these previous results, the radius of distribution that needs to be used. However the edge of contact surface might be subjected to boundary effect of the distribution.

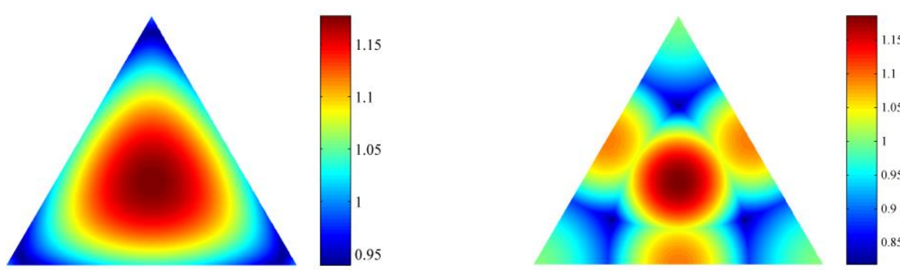

(a) 1st degree

(b) 2nd degree

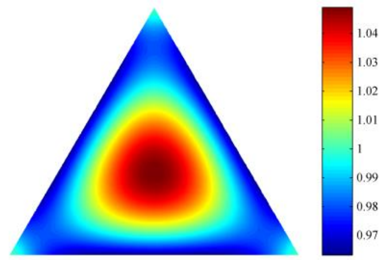

(c) 3rd degree

Figure 5: Weight factor distribution inside a triangle of three reduced contact nodes for several interpolation degrees. An equal force is applied on each node.

Interpolation degree	Radius (mm)	$\overline{\omega}$	σ
1	0.9501	1	0.0574
2	0.7425	0.9999	0.0835
3	0.9597	1	0.0234

Table 2: Weight factor computation results for several interpolation degrees: Optimal Radius, mean value ($\overline{\omega}$) and standard deviation (σ)

In the future, it could be interesting to have new capacities on the *DISTRIBUTING and *COUPLING cards to better distribute the forces on a given surface without forcing a reduction on an isometric grid.

3.2 Super-Element creation

The Super-Element creation can be summarized as follows: first of all, the reduced disc/pads contact interfaces (i.e contacts with a reduced number of nodes using *DISTRIBUTING and *COUPLING cards) are created on the Abaqus model. Then, a non-linear static analysis is performed on the Abaqus model with reduced contact interface and the displacements at the nodes retained for Super-Element creation are stored as reduced contact variables (contact force and gap). In a second step, contacts at disc/pads interfaces are deactivated but the displacements measured are still applied to the future reduction nodes with the "*Boundary, FIXED" parameter. In a third step, a frequency analysis is performed on 0-12kHz range. In the last step, a Craig & Bampton reduction is computed using the *SUBSTRUCTURE GENERATE. The *RETAINED NODAL DOFS card allows to specify the nodes used in the disc/pads contact interfaces to keep as reduction nodes. Except disc/pads contacts, all others contacts are linearized in this substructure generation. The mass and stiffness matrix of the Super-Element are exported by the *SUBSTRUCTURE MATRIX OUTPUT card. For this card, we regret that options “STRUCTURAL DAMPING MATRIX” and “VISCOUS DAMPING MATRIX” are not available. We would be interested by them.

3.3 Super-Element assembly

Concerning the Super-Element assembly, it may be noticed that Abaqus in no more used and all the computations are done thanks to Matlab software, as illustrated in Figure 2. This subsection details the method to compute the non-linear static step of the SE assembly at the exact static equilibrium.
The non-linear static system solved by Abaqus is described as follows:

Equation 1: $$\boldsymbol{K_{nl}(U_s)U_s + F_{nl}(U_s) = F_{ext}}$$

Where U_s corresponds to the static equilibrium position. F_{ext} represents the external force due to the external pressure applied to the piston and the caliper representing a brake operation. K_{nl} is the stiffness matrix due to the structural components and the Piston/Pad, Bracket/Pads and Caliper/Pad contact interfaces. F_{nl} contains the non-linear forces at the frictional interfaces between the disc and the pads.
As the Super-Element is created in a perturbation step, the system linearized around the static equilibrium can be written as follows:

Equation 2: $$\boldsymbol{K_{nl,U_s}U_s + F_{nl}(U_s) = F_{ext}}$$

where K_{nl,U_s} defines the linearized stiffness matrix at the vicinity of the static equilibrium U_s. All the contacts, except for the disc/pads interfaces, are linearized as a constant value in the stiffness matrix.

The local stability is studied introducing a perturbation ΔU around the static equilibrium:

Equation 3: $$\boldsymbol{K_{nl,U_s}(U_s + \Delta U) + F_{nl}(U_s + \Delta U) = F_{ext}}$$

Considering the Matlab implementation, the linearized system at the static non-linear equilibrium point is described in the following equation:

Equation 4: $$\boldsymbol{K_{nl,U_s}U_s + F_{matlab}(U_s) = F_{ext}}$$

where F_{matlab} corresponds to the non-linear contact as the disc/pads interfaces that will be described in the next section. K_{nl,U_s} is obtained thanks to the Super-Element creation in Abaqus. The only difference with Equation 2 is the way to compute the non-linear force involved in disc/pads contacts. According to the strategy defined above this contact is now a node to node contact between condensation nodes. As the calculated linearized equilibrium points for Abaqus software and Matlab software are the same, an equivalence of the contact force at the disc/pads interfaces for the non-linear equilibrium point has to be performed:

Equation 5: $$\boldsymbol{F_{matlab}(U_s) = F_{nl}(U_s)}$$

Considering experimental data, "Coudeyras, 2009" chose a cubic stiffness for the disc/pads non-linear contacts. For each contact node, its formulation is given in Equation 6 and Equation 7:

Equation 6: $$\boldsymbol{F_{matlab} = \begin{cases} k_l\delta + k_{nl}\delta^3 \; if \; \delta > 0 \\ 0 \; otherwise \end{cases}}$$

Equation 7: $$\boldsymbol{\delta = U_i - U_j}$$

where k_l and k_{nl} are respectively the linear and the non-linear stiffnesses and U_i and U_j the displacements of the coincident nodes i and j from the master and slave sides of the contact respectively. The subscript $matlab$ indicates that the non-linear forces computation is performed on the Matlab environment.

The main advantage of this choice is that this formulation is easy to linearize for further stability analysis. As said earlier we need to ensure the continuity in the contact force estimation between Abaqus and Matlab software. With two different contact formulations the only way to respect this constraint is to find an equivalent contact penetration for each node to node contact defined in Matlab in order to match the normal contact force value obtained with Abaqus software. Knowing the value of Abaqus normal contact force for each reduced node and the cubic stiffness parameters k_l and k_{nl}, it is easy to solve the following relation:

$$F_{matlab}(\delta + \xi) = F_{nl}(\delta)$$

where F_{nl} are the contact forces computed earlier with Abaqus software and δ the contact penetration associated to the static equilibrium point that has been previously estimated using Abaqus software. As said earlier this contact is computed using a linear penalty method in Abaqus software. Then the corrective term ξ in node to node contact penetration can be easily found.

4. Application for the reduced industrial model

This section presents the application of the reduction strategy defined above to the industrial brake model. The main objective of this section is to illustrate the efficiency of the proposed methodology to build a reduced Finite Element Model while keeping a good prediction on the three main instabilities observed on the reference Abaqus model.

4.1 Reduced models characteristics

To illustrate the effectiveness of the proposed strategy and discuss the impact of the size of the proposed reduction, several Abaqus models with several triangle size for disc/pads contact interfaces reduction will be investigated. Table 3 sums up the characteristics of the two models under consideration.

Abaqus models	Abaqus 104	Abaqus 212
Reduced contact nodes per pad	52	106
Total coincident nodes on disc volume mesh	104	212
Total references nodes for SE	210	526
Number of node to node contact elements	104	212

Table 3: Reduced models characteristics.

Figure 6 gives an insight of the reduced contact nodes layout over the pad surface. As point of comparison, the industrial Abaqus model contains 1370 nodes on the surface of each pad.

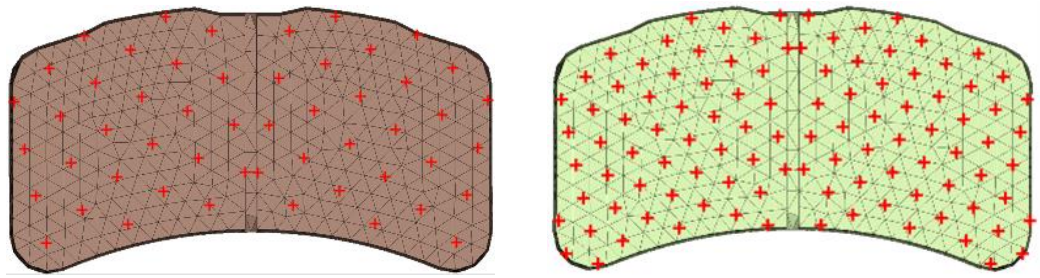

(a) 104 nodes (b) 212 nodes

Figure 6: Reduced contact nodes layout over the pad surface for several reduced model.

In the following of the study, both Abaqus models with reduced contact interface will be called Abaqus104 and Abaqus212 in reference to the number of reduced contact elements they contain.

4.2 Contact state resulting from a non-linear static analysis

As previously explained in "Sinou, 2004", the complex eigenvalue analysis is based on the determination of eigenvalues for the linearized system around the non-linear static equilibrium. The first step to evaluate the performance of the reduced contact interface is to compare some static quantities between the Abaqus reference and both reduced models (Abaqus104 and Abaqus212). In this paper, we just report the comparison between both reduced models and the reference model for the contact state when establishing the non-linear static equilibrium. So, a non-linear static analysis for a friction coefficient value of $\mu = 0.5$ (at the disc/pads interfaces) is computed. Figure 7 shows the results for both reduced models (i.e. Abaqus104 and Abaqus212, respectively). Contact state at each reduced node is represented by a circle (respectively by a plus sign) if the contact is open (respectively closed). Moreover, the contact map of the reference model is superimposed for each reduced models: the green and blue colors represent the closed and opened contact

As illustrated in Figure 7 (a-b), despite one or two nodes at the boundary between opened and closed contact zone the numerical, result for Abqus104 is consistent with those of the reference model. On Figure 7 (c-d), it clearly appears that the reduced model Abaqus212 is in perfect agreement with the reference model. This illustrates the fact that the number of nodes at the frictional contact interface can be drastically reduced in order to estimate the contact states by applying an appropriate strategy.

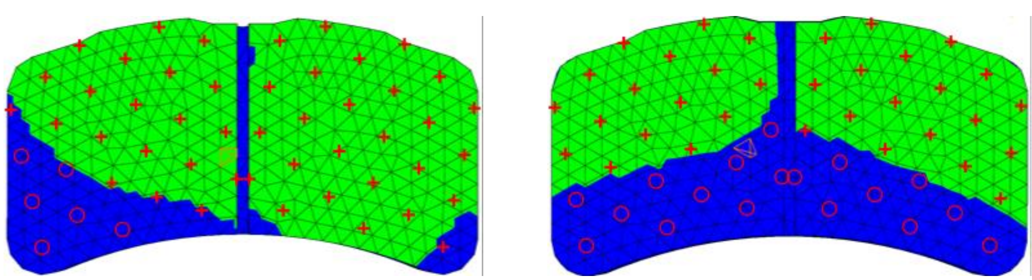

(a) (b)

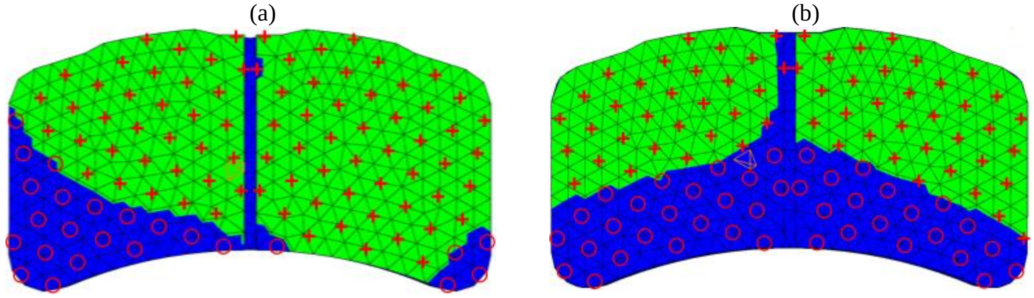

(c) (d)

Figure 7: Contact state comparison for each reduced model. The left column is for the inner pad and the right one is for the outer pad. (a)(b) Abaqus104 (c)(d) Abaqus212.

4.3 Stability analysis on the Super-Element assembly

Now we propose to illustrate the efficiency of the second part of the global strategy based on the Super-Element assembly.

As shown by “Fazio, 2015”, a Super-Element remains valid only at the vicinity of the non-linear static equilibrium point. More particularly, varying the friction coefficient at the disc/pads interfaces changes the static equilibrium on the Abaqus reference model. Then, a Super-Element is generated for each step of the friction coefficient (i.e. from $\mu = 0.1$ to $\mu = 0.9$ with a step size of 0.1). Real modes over 0-12kHz are kept for the Super-Element creation so that its validity can be assumed over 0-6kHz, our frequency range of interest. It represents a total of 135 modes. Next, a complex eigenvalue analysis is performed for each friction coefficient by using the associated Super-Element (SE) assembly. As illustrated in Figure 8, results for SE assemblies of both frequencies and real parts of the three unstable modes are in agreement with the reference (for Finite Element Model) even if a sudden rise in frequency of the third unstable mode starting at $\mu = 0.6$ can be noticed.

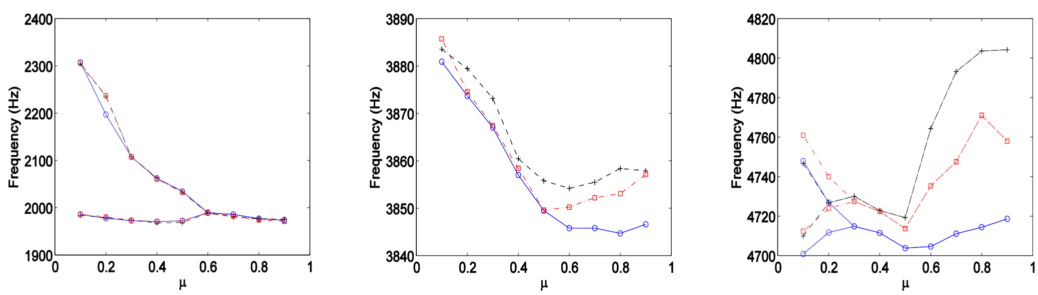

(a) (b) (c)

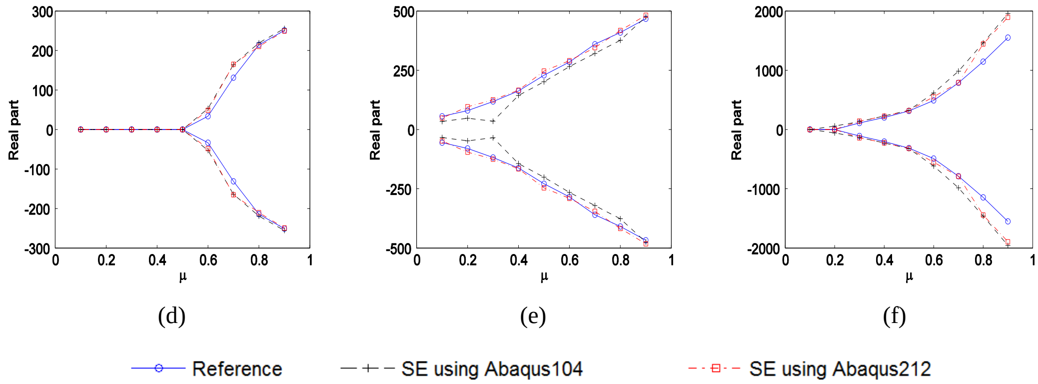

(d) (e) (f)

Figure 8: Evolution of the frequencies (a,b,c) and the real part (d,e,f) of the eigenvalues against the friction coefficient μ for the (a,d) 1.9kHz, (b,e) 3.8kHz and (c,f) 4.7kHz instabilities. A new Super-Element is generated at each μ for complex eigenvalue analysis on SE assembly.

In order to have a more detailed comparison of these SE assemblies (Matlab104 and Matlab212 which are respectively associated to Abaqus104 and Abaqus212), the mean error on the three instabilities of interest is estimated for all the values of the friction coefficient in the range of interest (i.e. from $\mu = 0.1$ to $\mu = 0.9$ with a step size of 0.1). The mean error is defined by:

$$\textbf{Equation 8: } \boldsymbol{\varepsilon_{tot}} = \sum_{j=1}^{M} \sum_{i=1}^{2} \frac{1}{2M} \frac{\left| f_{\mu_j,i}^{red} - f_{\mu_j,i}^{ref} \right|}{f_{\mu_j,i}^{ref}}$$

where μ_j corresponds to the value of the friction coefficient given by $\mu_j = 0.1 * j$.
Considering one instability, $f_{\mu_j,i}^{ref}$ (respectively $f_{\mu_j,i}^{red}$is the frequency of the i^{th} of the two modes that couple at the friction value μ for the Abaqus reference model (respectively reduced model). M stands for the number of friction coefficient for which a complex eigenvalue analysis is computed for the stability analysis. The minimum and maximum errors are also defined by

$$\textbf{Equation 9: } \boldsymbol{\varepsilon_{min}} = \min_{\mu_j} \sum_{i=1}^{2} \frac{1}{2} \frac{\left| f_{\mu_j,i}^{red} - f_{\mu_j,i}^{ref} \right|}{f_{\mu_j,i}^{ref}}$$

$$\textbf{Equation 10: } \boldsymbol{\varepsilon_{max}} = \max_{\mu_j} \sum_{i=1}^{2} \frac{1}{2} \frac{\left| f_{\mu_j,i}^{red} - f_{\mu_j,i}^{ref} \right|}{f_{\mu_j,i}^{ref}}$$

Finally, the mean error (given in Equation 8), the minimum and maximum errors (given in Equation 9 and Equation 10, respectively) are calculated for the SE assembly. We recall that this reduced model Abaqus104 was used for the SE generation. Results are given in Table 4 and Table 5. With this strategy the error never exceeds two percent whatever the unstable mode of interest.

In conclusion, these results illustrate the efficiency of the global strategy based on both nodal interface reduction and Super-Element generation.

Instability number	1	2	3
Matlab 104	0.19%	0.19%	0.88%
Matlab 212	0.19%	0.11%	0.52%

Table 4: Mean error on frequency for each pair of mode on the whole friction range between SE assembly and the reference model.

Instability number	1	2	3
Matlab 104	0%/1.77%	0.07%/0.36%	0%/1.89%
Matlab 212	0%/1.81%	0%/0.27%	0.21%/1.2%

Table 5: Min/Max error on frequency for each pair of mode between SE assembly and the reference model.

4.4 Limitation of a determinist point of view

For another model which is not detailed here, we notice that results are not all the time as good as those obtained previously.

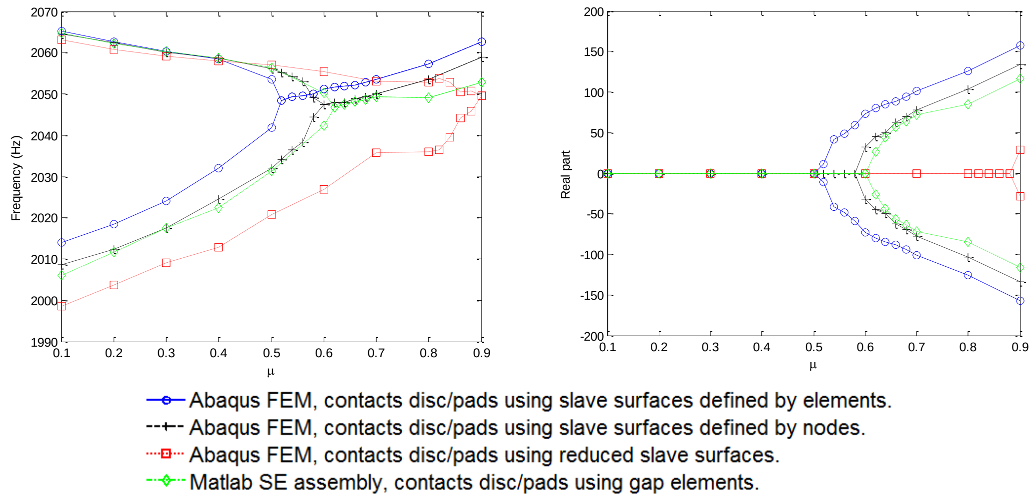

Figure 9 : Comparison of frequencies and reals parts for an instability and his conjugate according to the disc/pads contacts modeling. In the case of gaps, the Super-Element is used.

On Figure 9, the evolution of the frequencies and real parts are drawn for different approximations of disc/pads contacts. The first one, our reference, is a Finite Element Model (FEM) with a contact pair of type “node to surface” using surfaces of elements to define the slave surfaces. The second one consists simply to define the slave surfaces by groups of nodes extracted from the surfaces of elements. It is interesting to notice for this small modification that the effect on μ_{Hopf},the

coefficient of friction at Hopf bifurcation, is sensibly affected. The lower frequency of the conjugates modes is more affected than the other one. It's only an error of ~0.25%, but its leads to a delay of about 0.09 on μ_{Hopf} compared to the reference at ~0.51 (~17.5%). This result shows that some instabilities are sometimes very sensitive to the behavior at the contact interface. Then, approximations (interpolation and load transfer strategy) can lead to significant differences on μ_{Hopf} in some situations.
This sensitivity is still more important for the third approximation which is a Finite Element Model with disc/pads reduced contacts using 172 reduced nodes for pads. A softening effect of ~0.75% on the lower frequency leads to a difference of about 0.37 on μ_{Hopf} compared to the reference (~72.3%).
Then, for the Super Element assembly with 172 gap elements, which is the fourth approximation, a hardening effect of ~0.35% on the lower frequency is observed compared to the precedent case.
The softening effect of reduced contact was already observed by "Fazio, 2015", but not with such effects on μ_{Hopf}. The same for the hardening effect of Super Element Assembly. Perhaps the reduced contact could be improved using another strategy to distribute loads on the slave surface, to decrease edge effects for example. Nevertheless, real surface topology is not as perfect as the studied model. Then, another way could be to realize sensitivity analysis to compare models according to parametric uncertainties.

5. Conclusion

The global reduction strategy proposed by "Fazio, 2015", which is based on a nodal reduction, is proposed for an industrial non-linear brake system model. One of the advantages of the proposed strategy is based on an efficient contact reduction method for the disc/pads interfaces that allows a Craig & Bampton reduction to be used for further stability analysis. But as presented at the end, the sensitivity on the Hopf bifurcation can be very important in some cases. For these cases, it could be more appropriate to take uncertainties into account to compare results issue from reduced models with those from the Finite Element reference.
Based on these results, a future work could be to investigate effects of uncertainties. Another one will be to use reduced models to compute the self-excited vibrations.
Final number of variables on this reduced model is about 1500 for case with 212 reduced nodes for pads.
To finish, some evolutions are wished in Abaqus for future investigations: output on damping matrix for *SUBSTRUCTURE MATRIX OUTPUT and compatibility between *GAP and *MOTION cards. Moreover, dependent on agreement about PSA Peugeot Citroën patent, it could be interesting to have tools to build reduced contacts.

6. Acknowledgment

This work was achieved within PSA Peugeot Citroën Stellab program which allows to work with academics in openlabs, the VAT@Lyon openlab for NVH.

7. References

1. Abaqus Analysis User's Manual, Version 6.10, chapter 31 Constraints, Dassault Systèmes Simulia Corp., Providence, RI.
2. Brizard, D., Chiello, O., Sinou, J.-J., and Lorang, X., “Performances of some reduced bases for the stability analysis of a disc/pads system in sliding contact”, Journal of Sound and Vibration, 330(4):703--720, 2011.
3. Coudeyras, N., Sinou, J.-J., and Nacivet, S., “A new treatment for predicting the self-excited vibrations of nonlinear systems with frictional interfaces: The constrained harmonic balance method, with application to disc brake squeal”, Journal of Sound and Vibration, 319(3):1175--1199, 2009.
4. Craig, R. J., A review of time-domain and frequency domain component mode synthesis methods, International Journal of Analytical and Experimental Modal Analysis}, 2(2):59--72, 1987.
5. Fazio, O., Nacivet, S., Sinou, J.-J., « Reduction strategy for a brake system with local frictional non-linearities - Application for the prediction of unstable vibration modes”, Journal of Applied Acoustics, 91:12--24, 2015.
6. Loyer, A., Sinou, J.-J., Chiello, O., and Lorang, X., “Study of nonlinear behaviors and modal reductions for friction destabilized systems. application to an elastic layer”, Journal of Sound and Vibration, 331(5):1011--1041, 2012.
7. Sinou, J.-J., Thouverez, F., and Jezequel, L., “Methods to reduce non-linear mechanical systems for instability computation”. Archives of Computational Methods in Engineering: State of the Art of Reviews, 11(3):257-344, 2004.
8. Sinou, J.-J., “Transient non-linear dynamic analysis of automotive disc brake squeal - on the need to consider both stability and non-linear analysis”, Mechanics Research Communications, 37(1):96--105, 2010.
9. Vermot des Roches, G.,” Frequency and time simulation of squeal instabilities - Application to the design of industrial automotive brakes”, PhD thesis, Ecole Centrale Paris, 2011.
10. Villard, P., Nacivet, S., and Sinou, J.-J., “Superelement reduction of industrial finite element brake system for a constrained harmonic balance method”, INTER-NOISE and NOISE-CON Congress and Conference Proceedings, pages 3142--3151, 2012.